applied sciences

MDPI

Article

Study of Surface Emissions of ^{220}Rn (Thoron) at Two Sites in the Campi Flegrei Caldera (Italy) during Volcanic Unrest in the Period 2011–2017

Fabrizio Ambrosino [1], Carlo Sabbarese [2,3,*], Flora Giudicepietro [4], Walter De Cesare [4], Mariagabriella Pugliese [2,5] and Vincenzo Roca [2]

1 Department of Agricultural Sciences, University of Naples "Federico II", 80055 Portici, Italy; fabrizio.ambrosino@unicampania.it
2 National Institute of Nuclear Physics, Naples Section, 80126 Napoli, Italy; pugliese@na.infn.it (M.P.); vroca222@gmail.com (V.R.)
3 Department of Mathematics and Physics, University of Campania "L. Vanvitelli ", 81055 Caserta, Italy
4 Istituto Nazionale di Geofisica e Vulcanologia, Osservatorio Vesuviano, 80124 Napoli, Italy; flora.giudicepietro@ingv.it (F.G.); walter.decesare@ingv.it (W.D.C.)
5 Department of Physics, University of Naples "Federico II", 80126 Napoli, Italy
* Correspondence: carlo.sabbarese@unicampania.it

Abstract: The study concerns the analysis of ^{220}Rn (thoron) recorded in the surface soil in two sites of the Campi Flegrei caldera (Naples, Southern Italy) characterized by phases of volcanic unrest in the seven-year period 1 July 2011–31 December 2017. Thoron comes only from the most surface layer, so the characteristics of its time series are strictly connected to the shallow phenomena, which can also act at a distance from the measuring point in these particular areas. Since we measured ^{220}Rn in parallel with ^{222}Rn (radon), we found that by using the same analysis applied to radon, we obtained interesting information. While knowing the limits of this radioisotope well, we highlight only the particular characteristics of the emissions of thoron in the surface soil. Here, we show that it also shows some clear features found in the radon signal, such as anomalies and signal trends. Consequently, we provide good evidence that, in spite of the very short life of ^{220}Rn compared to ^{222}Rn, both are related to the carrier effect of CO_2, which has significantly increased in the last few years within the caldera. The hydrothermal alterations, induced by the increase in temperature and pressure of the caldera system, occur in the surface soils and significantly influence thoron's power of exhalation from the surface layer. The effects on the surface thoron are reflected in both sites, but with less intensity, the same behavior of ^{222}Rn following the increasing movements and fluctuations of the geophysical and geochemical parameters (CO_2 flux, fumarolic tremor, background seismicity, soil deformation). An overall linear correlation was found between the $^{222-220}$Rn signals, indicating the effect of the CO_2 vector. The overall results represent a significant step forward in the use and interpretation of the thoron signal.

Keywords: ^{220}Rn; volcanic unrest; hydrothermal alteration; CO_2; anomaly and trend; Campi Flegrei

Citation: Ambrosino, F.; Sabbarese, C.; Giudicepietro, F.; De Cesare, W.; Pugliese, M.; Roca, V. Study of Surface Emissions of ^{220}Rn (Thoron) at Two Sites in the Campi Flegrei Caldera (Italy) during Volcanic Unrest in the Period 2011–2017. *Appl. Sci.* **2021**, *11*, 5809. https://doi.org/10.3390/app11135809

Academic Editor: Stuart Hardy

Received: 20 May 2021
Accepted: 21 June 2021
Published: 23 June 2021

1. Introduction

The isotope ^{220}Rn (also thoron) is the by-product of the natural decay of ^{224}Ra that is derived from the decay series of ^{232}Th. Its half-life is 55.6 s. It is one of the isotopes of radon noble gas, second in abundance only to ^{222}Rn [1,2]. The latter has a half-life of 3.82 days, coming from the decay of ^{226}Ra in the ^{238}U series. Radon naturally occurs in the Earth's crust. It is currently used by the scientific community as one of the most monitored gases on Earth for tracing of natural phenomena (seismo-tectonic and volcanic activity) linked to soil degassing along faults, fractures and crustal discontinuities [1,3]. Usually, in these contexts, ^{222}Rn is transported over great distances thanks to its long half-life, and its variations are linked to deep phenomena of the Earth's crust. The ^{220}Rn measured on the

surface, on the other hand, is produced only locally due to its much shorter half-life, so it cannot provide information on remote processes as its variations are due to local effects. The exhalation of radon/thoron from materials containing the parents is influenced by external factors, which can also act at a distance from the measuring point. In this way, the measure of the thoron activity produced locally can be correlated with the deep source.

Radon generation and migration in the environment has been seen to depend on many factors: the porosity and permeability of the bedrock, the nature of the fluid transporting radon (i.e., carrier gases), increase due to weathering and chemical–physical alteration processes [4–6]. Furthermore, the effectiveness of radon release from minerals or radon emanation is contingent upon the specific surface area of the minerals, their size and shape and the presence of imperfections [7,8]. Within this framework, many studies have investigated the analysis of radon time series with the aim of identifying anomalies and extracting anomalous seasonal trends. Radon anomalies of non-tectonic origin have been reported to be very similar to those of seismo-tectonic origin, where strong crustal deformative processes and high heat flows are recognized [9–11]. Other ones reported the physico-chemical phenomena in volcanic geothermal areas as possible mechanisms to explain the anomalous increase in radon signal in soil and groundwater [1,6,12]. The common aspect is that the radon measurement can provide useful information if it is continuously recorded at a site, where the half-lives of the radon isotopes play a key role; the half-life of ^{220}Rn makes the distance that it can travel, from its source site within the rock and filtrate through the ground and through cracks, before undergoing radioactive decay, much shorter than that traveled by ^{222}Rn in the same medium [2,13]. This fact can provide information on soil gas sources: deep soil layers for ^{222}Rn and shallow soil layers for ^{220}Rn [2,6]. Thus, the contribution of ^{220}Rn is usually negligible compared to that of ^{222}Rn. However, in some cases high levels of thoron activity concentration can be found in weakly ventilated areas where advective transport of soil gas is particularly high and/or rich in rocks containing significant amounts of ^{232}Th-rich mineral phases [13]. For these reasons, the literature is replete with ^{222}Rn measurement in soil and surface water as a tool to monitor geophysical events (earthquakes, seismotectonic activity and volcanic activity), while only few studies have fully reported thoron measurement for the same application. In general, the investigation on ^{220}Rn in the literature is lacking [14,15]. The main studies deal with laboratory experiments that aimed to develop a thoron reference for in air measurement systems [2,16]. The remaining few studies focus on soil gas ^{222}Rn–^{220}Rn isotope pair measurements in underground environments (caves, mines), where significant concentration levels of thoron can be detected [3,13,17]. There is a lack of papers concerned with thoron alone for geophysical purposes, despite the fact that interest in thoron monitoring has grown considerably in recent years and is still increasing.

The present study focuses on the analysis of soil gas ^{220}Rn activity concentration time series at two different sites of the Campi Flegrei caldera (Naples, Italy), over a period of about seven years, from 1st July 2011 until 31st December 2017. The gas was continuously monitored with systems based on the electrostatic collection, and the subsequent spectrometry analysis, of the α-particles of ^{220}Rn daughters. The two sites were located in: *i.* Monte Olibano (OLB), inside a disused railway tunnel into the central area of the caldera; and *ii.* Monte Sant'Angelo (MSA), outside the Department of Physics "E. Pancini" of the University of Naples "Federico II" [18] (Figure 1). This work retraces the analyses performed in [1] on the soil gas ^{222}Rn activity concentration time series at the same two sites, which concluded that the ^{222}Rn follows the evolution of the Campi Flegrei caldera, in agreement with the more classic geophysical and geochemical parameters routinely used [19,20].

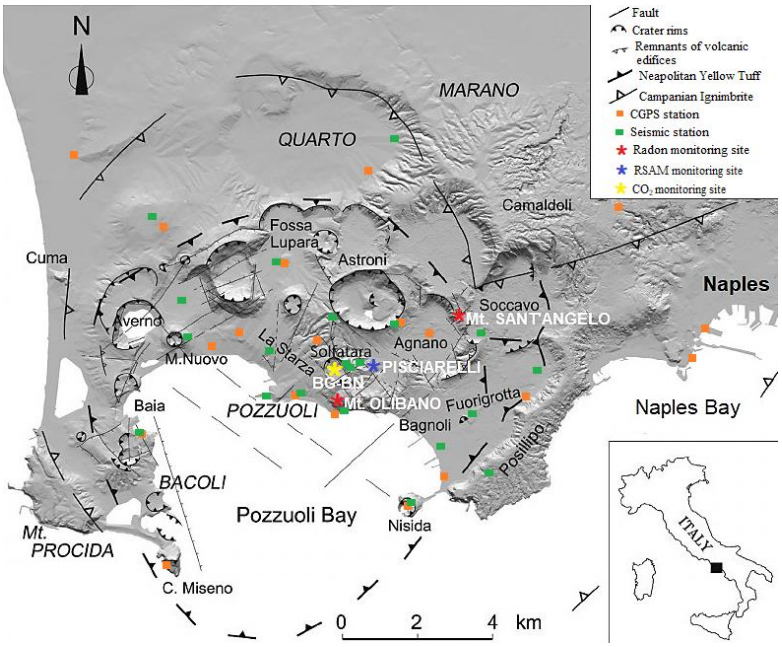

Figure 1. Map of the Campi Flegrei caldera (Naples, Italy) from [1,18]. The map shows the structural setting of the caldera characterized by tectonics and volcano-tectonic activity. The two radon monitoring sites of Monte Olibano and Monte Sant'Angelo, and the other monitoring sites of geochemical and geophysical parameters are reported.

Campi Flegrei is a caldera located on a NE–SW-trending structure in the Campanian Plain, occupying an area of about 120 km^2. This area consists of an interesting geological system characterized by interaction between tectonics and volcano-tectonic activity, with NE–SW- and NW–SE-trending faults that control the distribution of volcanic centers [1,20]. In the last two decades, the caldera has been subject to a long-term volcanically induced crisis, still ongoing, characterized by numerous episodes of ground uplift with seismic activity, an increase in the acceleration of the deformation of the soil due to magma intrusion at shallow depth and large emission of hydrothermal–volcanic and geothermal fluids through soil diffuse degassing and fumarolic vents [21,22]. The complete description of the structural geological setting of the Campi Flegrei caldera, and its current unrest phase from a geophysical and geochemical point of view, can be found in the literature [20,23].

The analysis of the ^{220}Rn time series at the OLB and MSA sites is performed using a well-proven hybrid method, successfully applied for the trends and residuals (anomalies) extraction [1,24–26]. The hybrid method optimally combines standard techniques for the signal decomposition to filter the known and unknown seasonal/periodical components out, and a technique for the forecasting and reconstruction of the time series in order to obtain the anomalies as differences with the raw signal [11,25]. Here, the trends and the anomalies of the thoron time series at OLB and MSA are compared with the main geo-parameters monitored during the Campi Flegrei caldera unrest: CO_2 flux, fumarolic tremor, background seismicity, ground deformation and temperature and pressure of the hydrothermal system [20]. The goal of this study is the demonstration that thoron present in the surface layer, despite its very short life, may be influenced by deep mechanisms of the evolution of the volcanically induced crisis of the Campi Flegrei caldera over the period 1 July 2011−31 December 2017, as well as the ^{222}Rn isotope [1]. However, aware of the limits of this radioisotope, we do not want to use it instead of radon and other gases that provide a broader understanding of volcanic environments. We will, however, highlight the particular characteristics of thoron in the surface soil in a particular volcanic area, where its exhalation rate is influenced by external factors, which can also act at a distance from the point source.

2. Materials and Methods

2.1. Monitoring Data

The monitoring data used in the present work were: ^{220}Rn (thoron) activity concentration, fumarolic tremor, background seismicity, ground deformation, CO_2 air concentration flux and the temperature and pressure of the hydrothermal system (Figure 1).

The ^{220}Rn activity concentration (Bq/m^3) monitoring was carried out by continuous measurements in the soil gas of Campi Flegrei caldera, at Monte Olibano and Monte Sant'Angelo sites. Monte Olibano (OLB) is inside a disused railway tunnel into the central area of the caldera; while Monte Sant'Angelo (MSA) is outside the Department of Physics 'E. Pancini' of the University of Naples "Federico II" [27]. The ^{220}Rn measurements were performed by electrostatic collection of the ionized descendants of the gas (^{216}Po, ^{212}Po and ^{212}Bi) on a Silicon detector inside a cylindrical metallic chamber [28]. The monitor used was the RaMonA® system, able to distinguish and observe weak signals, e.g., from the ^{220}Rn, in the presence of a lot of background noise due to ^{220}Rn [29]. The complete alpha spectrum of ^{220}Rn and ^{222}Rn was analyzed by FORTAS® software, which allows the adequate discrimination of thoron and radon progeny by deconvolution fitting processes with high accuracy [30]. The soil gas was 1 L/min pumped gas from a depth of 0.80 m to the inlet of the metallic chamber. This air inlet position allowed relatively constant environmental processes. The time interval of detected and processed data was 1 h, but the daily average of the data was used in the analysis. The same methodology was also used to monitor the ^{222}Rn, using ^{218}Po and ^{214}Po descendants [1]. The device also monitored temperature, relative humidity and pressure inside the detection chamber and in the surface soil of the measurement site. The detailed description of the entire process of ^{220}Rn monitoring can be found in [29,30].

The fumarolic tremor measures seismic changes in ground vibration, in m/s, in real time (real-time seismic amplitude measurement-RSAM). A characteristic RSAM value was computed daily by assuming as representative the minimum value registered during the night, corresponding to the time of the day when anthropogenic noise is lowest (lower than during daylight hours). It was monitored by a 3-component seismometer located at the Pisciarelli fumarole. Analytical methodologies and uncertainties are described in [31–33]. The background seismicity refers to the cumulative distribution of Campi Flegrei seismicity, which simply corresponds to the sum of the days in which at least one earthquake occurred. The reference station for Campi Flegrei seismicity is located close to the Pisciarelli hydrothermal area where the post-2000 seismicity focuses. A full description of the Campi Flegrei seismic network is reported in [23,32]. Ground deformation data (cm) represent the maximum vertical displacement acquired by the GPS network, which provided measurements of the 3D time changes in stations operating at Campi Flegrei. A full description of the GPS network is reported in [32,33]. The CO_2 concentration flux (µmol/mol) from Pisciarelli vent was monitored by systematic sampling. The analytical methods and their uncertainties are available in [19,34]. The trend of CO_2 flux, used in this work, was computed by applying the EMD method (see Section 2.2). The temperature and pressure of the hydrothermal system was estimated by applying a gas-equilibria approach applied to the hottest fumaroles of Campi Flegrei. The details are in [35].

2.2. Time Series Analysis

The analysis of the ^{220}Rn time series was performed by the well-proven hybrid method Multiple Linear Regression + Empirical Mode Decomposition + Support Vector Regression (MLR + EMD + SVR) [11,24,27], already used for the analysis of the ^{222}Rn signal in the retraced paper [1]. It is an effective methodology that aggregates multiple separate methods, combining the performance advantages of each one, optimizing algorithms and achieving greater accuracy, developed and tuned in the Matlab® environment [25,36]. The signal trend extraction was performed by using the MLR + EMD method. The MLR technique creates a model describing the contribution of the recorded environmental parameters (i.e., temperature, relative humidity and pressure, which influence the signal) to the time series,

via a multiple linear regression model based on the least-squares fit. The original time series was subtracted by the MLR model, in order to obtain the correct one. The procedure is fully described in [37]. On the correct time series, the EMD technique was applied to further filter the unknown seasonal–periodic modulations out of the signal, by decomposition. The signal was decomposed into a collection of components; they were obtained by iterative differences between the signal and the average of the upper and lower envelopes, which came from the spline interpolation among all the local maxima and minima, respectively. The components increased progressively in frequency, and the decomposition process ended with constancy or monotony of the signal. The last component was the representative trend of the time-series. The detailed analytical description is reported in [38,39]. The EMD method is improved to deal with time series having missing data, thanks to the Self-Consistent Regression Estimator (SCRE) technique that recursively imputes missing values [40]. The residuals (anomalies) identification was performed by observing the raw signal outside the two 95% confidence intervals (CI) of the forecasted signal, obtained using the SVR technique applied to the sum of all components output of MLR + EMD hybrid method [1,24]. The SVR method computes the forecasted signal through a regression model using the set of data as training, in order to predict them with a function having lowest deviation. The regression model was made by using the Gaussian kernel mapping function with the Lagrange dual formulation. A complete analytical description of the SVR method is available in [41,42], with explanatory examples. The residuals (anomalies) were recognized if they were beyond one of the two forecasted time series at 95% CI that contained the same raw signal, and, then, were computed by subtracting the two forecasted time series from the raw one, in absolute terms. The anomalies identification process, with many exemplifying figures, is in [1,24,26,43,44].

3. Results

The analysis of our recorded ^{220}Rn time series in soils within the Campi Flegrei caldera area was performed using the sequential application of separate signal processing methods (together forming a hybrid method), described in Section 2.2, focused on the recognition of the trends and the possible residuals (anomalies) of the signals [36,45–47].

The daily time series of ^{220}Rn activity concentration in soils, over the period 1 July 2011–31 December 2017, are displayed in Figure 2a,b for OLB and MSA sites, respectively. The same figure also reports the ^{222}Rn (hereafter also radon) activity concentration time series, taken from [1], with the aim to highlight the differences in the recorded signals of the two isotopes of the noble gas.

All four signals were corrected for the recorded influence of outside driving forces, i.e., temperature, relative humidity and pressure, through the Multiple Linear Regression (MLR) technique [37]. This means that the influences of those driving forces were filtered out from radon and thoron signals. The occasional lack of data in the time series was treated with the Self-Consistent Regression Estimator (SCRE) technique that recursively imputes missing values [40]. As carried out in [1] for the ^{222}Rn time series, here the ^{220}Rn time series was investigated with the Empirical Mode Decomposition (EMD) for distinguishing and extracting the different components and trends [46]. Most of the components obtained by applying the EMD method (not showed for brevity) are due to meteorological and seasonal phenomena. The trend is the last component obtained by EMD, which represents the smooth component containing information about time series global change [24].

The residuals (i.e., anomalies) refer to those values not attributable to the normal evolution of the studied time series [45]; here, they were recognized as the values of the ^{220}Rn time series out of the 95% confidence interval (95% CI) of the differences between the measured signals and the forecasted time series [1,43]. The forecasted time series was computed by the application of the forecasting Support Vector Regression (SVR) method on the sum of the previous components obtained from EMD method [42].

The residuals (anomalies) and the trends of ^{220}Rn time series at OLB and MSA are shown in Figure 3a,b, respectively, together with the same ones obtained for ^{222}Rn from [1].

The trends (Figure 3b) underline an increasing pattern of ^{220}Rn activity concentration during the entire monitoring period at both OLB and MSA sites with different intensity, as well as in the ^{222}Rn trends. Instead, thoron residuals concentrate in four well-defined periods (March–November 2013, May–September 2014, April–November 2015 and August 2016–December 2017; Figure 3a). The ^{222}Rn residuals concentrate in about the same four periods. It is interesting to note how the $^{222-220}$Rn residuals occur almost simultaneously at both sites, even if with different intensity. The different intensity of the residuals and trends of ^{222}Rn, and here also manifested in the ^{220}Rn, lower in MSA than in OLB, was already explained in [1], as a consequence of the different distance of $^{222-220}$Rn stations from the center of the current unrest that roughly coincides with the central area of the Campi Flegrei caldera (~1 km for OLB and ~4 km for MSA, Figure 1), where the hydrothermal activity is concentrated and where the maximum ground uplift and the highest seismicity are recorded. The same explanation can therefore be assumed for the thoron results. In addition, comparing the radon–thoron results in Figure 3, a new consideration emerges from the present study; the intensity of thoron trends are almost halved, while the residuals are three times less, with respect to those of radon, in both monitoring sites. This aspect has a double natural concurrence of causes: the possible less abundant presence of ^{232}Th sources in the soils of Campi Flegrei area, and/or, more likely, the difficulty of ^{220}Rn emission from the sub-surface into air, due to its minimum half-life of a few seconds, with respect to ^{222}Rn that manages to be outgassed more easily, with a half-life of some days.

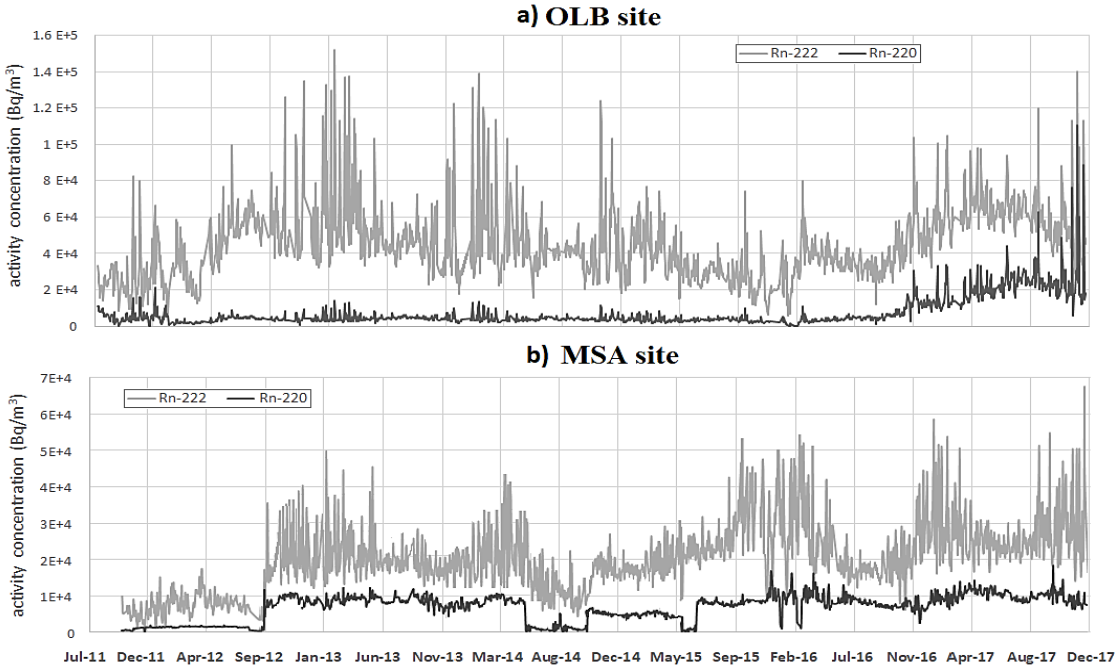

Figure 2. Thoron (^{220}Rn) and radon (^{222}Rn) activity concentration time series recorded at OLB (**a**) and MSA (**b**) sites, from 1 July 2011 up to 31 December 2017. The signals were corrected for the meteorological influences with the MLR method. Lack of data was filled with the SCRE technique. The steep jumps in thoron signal at MSA mean unexpected failure of the data logging network.

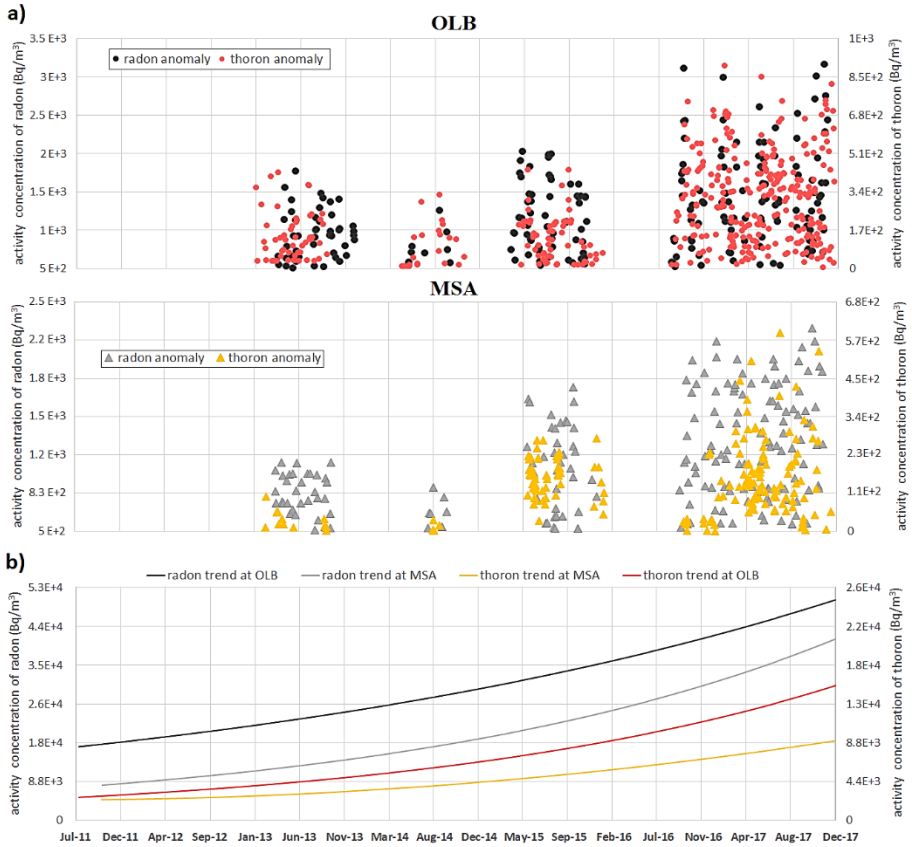

Figure 3. (**a**) Anomalies of $^{222-220}$Rn at OLB (first graph) and MSA (second graph) sites, obtained by subtracting the forecasted signals, using hybrid method MLR + EMD + SVR, from the raw recorded data, within a 95% CI. (**b**) Trends in $^{222-220}$Rn at OLB and MSA sites, obtained by applying the MLR + EMD hybrid method. The accuracy of the measured data, i.e., the error bars, is an approximately constant 4%.

4. Discussion

The obtained results of trends and residuals of ^{220}Rn in soils of OLB and MSA sites were compared to independent geo-indicator data used to depict the current phase of Campi Flegrei volcanic unrest, during the period 2011–2017 (Figure 4), characterized by ground uplift, increasing seismic activity and marked variation in the hydrothermal activity and geothermal fluid degassing.

In particular, we considered the following data sets: (i) the ground deformation data synthetically represented by the maximum vertical displacement acquired by GPS networks [32]; (ii) the cumulative number of days with earthquakes since 2000, i.e., the background seismicity [32]; (iii) the major fumarolic tremor (RSAM) registered by the seismic station at of Pisciarelli fumarole [33]; (iv) the trend of CO_2 air concentration flux from Pisciarelli vent [6]; and (v) the temperature and pressure of the hydrothermal system [48]. As demonstrated by previous works in [20–23,32,33,48], the presently investigated geophysical–geochemical parameters are recognized as powerful indicators of the current unrest in the Campi Flegrei caldera. Fumaroles are in fact known to generate seismic tremors, which correlate with the variations in the ground shaking/deformation and in hydrothermal activity, controlled by the gas fluxes from the fumarolic vent, such as CO_2 concentration flux in air. From the comparison in Figure 4a, the thoron residuals (anomalies) at OLB and MSA sites mimic the prominent fumarolic tremor enhancement peaks, which practically coincide with the periods of highest seismic tremor of the hydrothermal area. This finding is especially significant, because the RSAM signal is directly controlled by the Pisciarelli emission. Figure 4b shows the correlation of the thoron trends at OLB and MSA sites with the following signals registered at Campi Flegrei caldera: ground deformation,

the background seismicity and the trend of CO_2 air concentration flux computed in [6]. Actually, all these signals demonstrate a general similar increasing pattern.

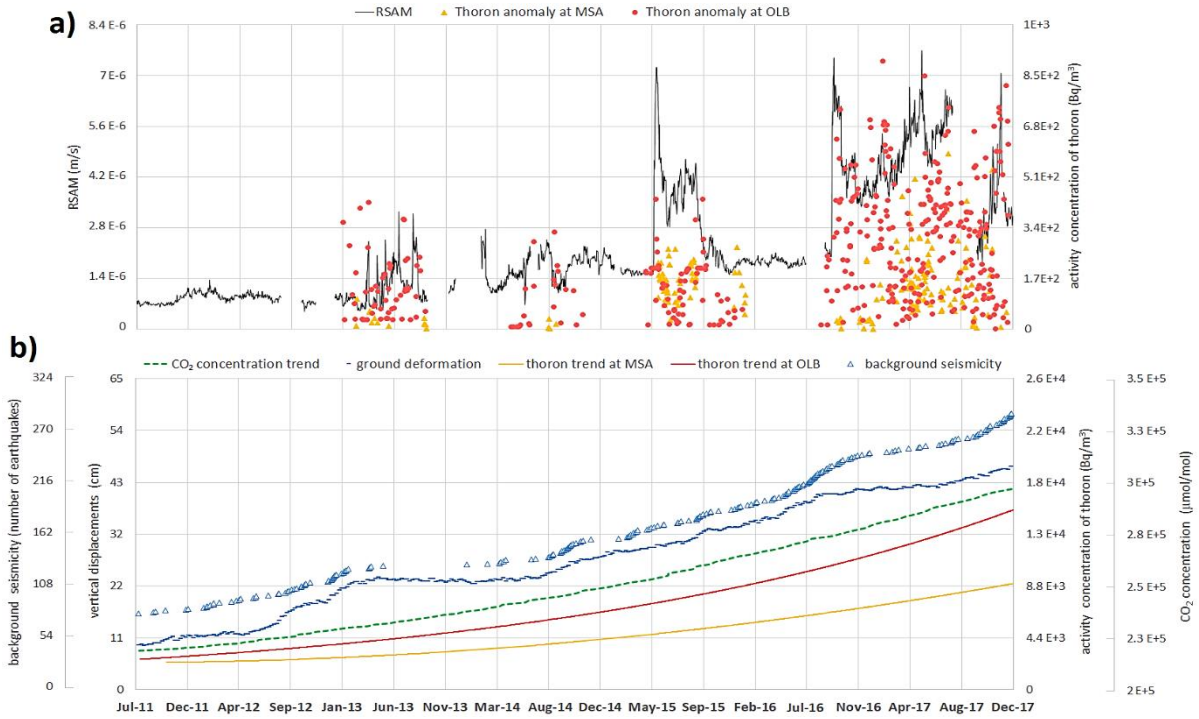

Figure 4. (**a**) Thoron residuals (anomalies) at OLB and MSA sites compared with the fumarolic tremor (RSAM) registered at Pisciarelli fumarole. (**b**) Thoron trends at OLB and MSA sites compared with the maximum vertical displacement at Campi Flegrei, the background seismicity (i.e., the cumulative number of days with earthquakes since 2000) and the hydrothermal CO_2 flux trend from Pisciarelli vent. The accuracy of the measured data, i.e., the error bars, is an approximately constant 4%.

The results in Figure 4 suggest the high influence that the main geo-indicators of the current crisis at Campi Flegrei have on the thoron in the surface layer of the soil. Independently from the generation–propagation mechanisms of all the observed signals, they appear to be linked together. During long-term periods of volcanically induced crisis, characterized by continuous injections of magma that stall at very shallow levels, a volcano system passes through different stages of hydrothermal activity and degassing phenomena [49]. The dynamic changes in gas flow regime within the Campi Flegrei caldera system influence the RSAM signal, controlled by the Pisciarelli emission [50]. In particular, the increasing CO_2 degassing of Pisciarelli vent affects the increase in the fluid pressure (Figure 5b) of the Campi Flegrei hydrothermal system [19,48]. Thus, the deformation of the soil and episodes of ground uplift, accompanied by correspondent seismic activity, grows, inducing an increase in the permeability and porosity of the media [32,35,51] that can induce an increase in the release of thoron on the surface and, therefore, the growing trend. Indeed, the CO_2 plays a key role in this process in controlling the migration and the transport of gas traces, such as ^{220}Rn and ^{222}Rn, towards the surface [52–54]. The variation in CO_2 fluxes can explain the wide range of soil ^{220}Rn activity concentration, from surface ground layers (<1 m) to migrated out into the atmosphere.

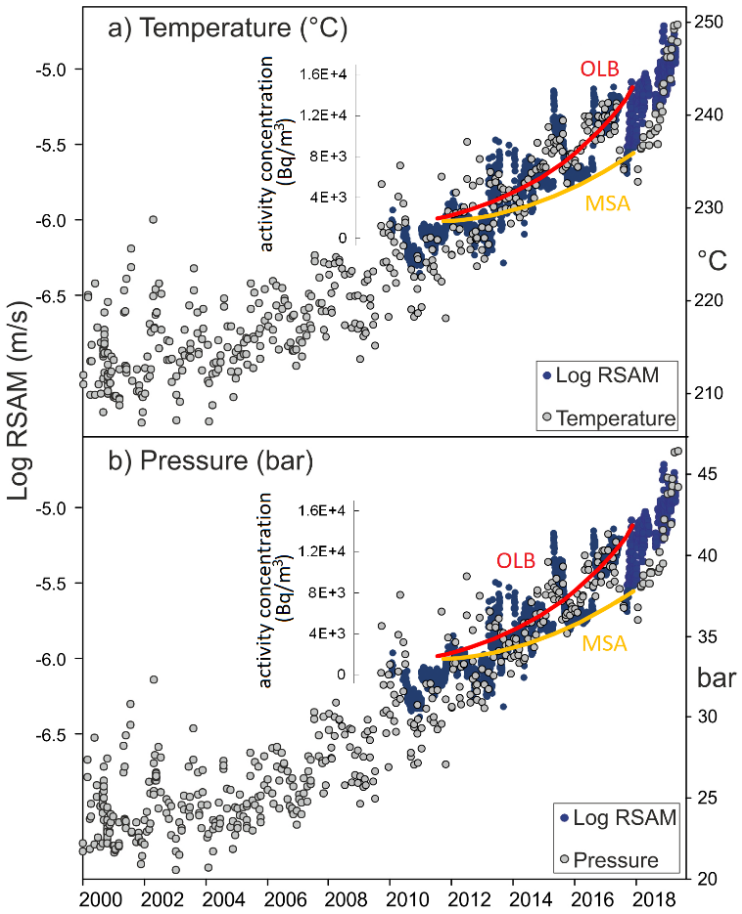

Figure 5. Comparison of temperature (**a**) and pressure (**b**) of the Campi Flegrei hydrothermal system, estimated at Pisciarelli fumarole, with the fumarolic tremor (RSAM) registered at Pisciarelli fumarole and with thoron trends at OLB and MSA sites.

This explanation of the concatenation of interrelated geophysical and geochemical events moved by pressure gradients, however, cannot fully explain the outgassing range of ^{220}Rn from the surface ground, considering the very short half-life of the ^{220}Rn, which makes escape from its point source within the rock and filtrate through the ground into the atmosphere very difficult. Therefore, to shed light on such anomalies and trends observed in the present work, two recent papers [55,56] come to our aid, which both experimentally proved the increase in Rn (both isotopes) emanating power induced by thermal gradients due to magma dynamics in active volcanic areas [57]. Such a result is particularly true in volcanic areas where intense hydrothermal alteration is present, such as at the Campi Flegrei caldera [23,58]. Progressive phenomena of increasing temperature can produce surface ^{220}Rn emissions even almost four orders of magnitude higher than those measured during rock deformation, micro-fracturing and failure [56]. Thermal gradients can contribute significantly to produce, superficially, ^{220}Rn emissions spatially heterogeneous and non-stationary in time, resulting in a transient state dictated by temperature gradients and the carrier effects of gases [55]. Thus, the increase in thoron emanation coefficient may lead to higher and anomalous concentrations of thoron in surface soil gas [55,59]. In our case, this phenomenon caused by thermally induced reactions on the thoron signal is demonstrated in Figure 5a, where the increasing pattern of the temperature of the Campi Flegrei hydrothermal system [20,35,50], which strongly characterizes the fumarolic activity (RSAM) of the caldera [48], well matches with the increasing trend of the thoron at OLB and MSA sites. In [55], it is stated that positive ^{220}Rn anomalies in surface soils of active volcanic areas are addressed to repeated cycles of stress due to increasing thermal pressures, leading to the opening or reactivation of fractures and to changes in rocks as a function of

temperature. Actually, this is what we assumed to occur in the Campi Flegrei hydrothermal system (Figure 4a).

Taken together, all the different independent signals that we have discussed are likely affected by the significant rise in temperature and pressure of the hydrothermal system at the Campi Flegrei caldera, which began two decades ago and is still ongoing [18,33] (Figure 5). In these scenarios, the temperature increase may induce thermal devolatilization phenomena on surface thoron emission and the fluid pressure may increase, favoring ground deformation, earthquakes and the flux of the hydrothermal gas [1]. Thus, these hydrothermal alterations, induced by increases in the temperature and pressure, frequently modeled in terms of enhanced heat flow with related stream discharge and stress-induced micro-fracturing with an increase in porosity and permeability, act as perturbation mechanisms that contribute to produce anomalies in surface thoron outgassing, spatially heterogeneous and non-stationary in time [55,60]. In addition, the carrier effects due to CO_2 fluxes may further contribute to thoron emission [52]. In brief, hydrothermal alteration of the caldera occurs on the surface soils and, here, the thoron, normally outgassed from rock, is influenced, producing increasing emissions, also sustained by CO_2 [61].

Alteration of temperature and pressure within the Campi Flegrei hydrothermal system also reflects the variation in gradients of temperature and pressure recorded at the nearby Rn stations, which show a high correlation factor (>0.7) with Rn activity concentration.

The same comparisons in Figures 4 and 5 were made in [1] for the ^{222}Rn signals, at both sites and over the same period. Almost the same correlations were found among the different independent signals, and quite similar conclusions were also drawn. Thus, the surface emission of ^{220}Rn behaves like ^{222}Rn emission, both influenced by geo-indicators of the evolution of the current volcanically induced unrest of the Campi Flegrei caldera. The different intensities of trend curves and residuals, lower in MSA than in OLB, occurring equally for ^{222}Rn and ^{220}Rn, are likely due to the different distances of the two sites from the main active degassing area, i.e., Pisciarelli fumarole, the center of the current unrest of the Campi Flegrei caldera, where the hydrothermal activity is concentrated [35] (Figure 1). Therefore, the intensity difference of the surface ^{220}Rn signals can be well explained by variation in the flux of the hydrothermal–volcanic CO_2 carrier gas, lower in MSA with respect to the higher effect in OLB, which is located inside the central unrest area. This result suggests the extension of the area affected by the current Campi Flegrei crisis, larger than the area of seismicity and of intense hydrothermal activity [1].

Figure 6 shows the activity concentration values of ^{222}Rn versus those of ^{220}Rn, at the OLB (Figure 6a) and MSA (Figure 6b) sites during the entire monitoring period of 2011–2017. The two graphs testify a linear correlation between the gas isotopes (R^2 is 0.65 for OLB and 0.54 for MSA), which most likely means that they have been carried out by the venting of CO_2 gas, favored by crustal stress/strain changes [53,62]. Two enlargement sides are also evident in Figure 6, indicating that different gas sources are needed to explain the Rn data. A lower part, that exhibits radon–thoron values of almost the same order of magnitude, can denote Rn variations more sensitive to the shallower sources at lower activity concentration level [62]. In contrast, a higher part, that shows low thoron values corresponding to significant and high radon values, naturally indicates ^{222}Rn coming from deep sources compared to ^{220}Rn only from shallow sources (ground surface) [62].

This fact intuitively suggests that a certain amount of ^{220}Rn comes from natural outgassing at the surface, and it is not carried by CO_2 gas together with the ^{222}Rn, probably coinciding with periods of less, quiet and moderate hydrothermal and seismic activity. The scattered graph of the data from MSA in Figure 6b, compared to the clustered one from OLB in Figure 6a, underlines two important aspects. The first one is the substantial difference in the two signals at MSA and OLB, differently influenced by the local meteorological parameters, due to the location of the Rn stations; outside at MSA was the most influenced, with respect to the OLB site inside a gallery [27,37]. The second aspect is the distance of both sites with respect to the central area of the current unrest of the Campi Flegrei caldera, which is closer to OLB than to MSA, which markedly influences $^{222-220}$Rn emissions [1].

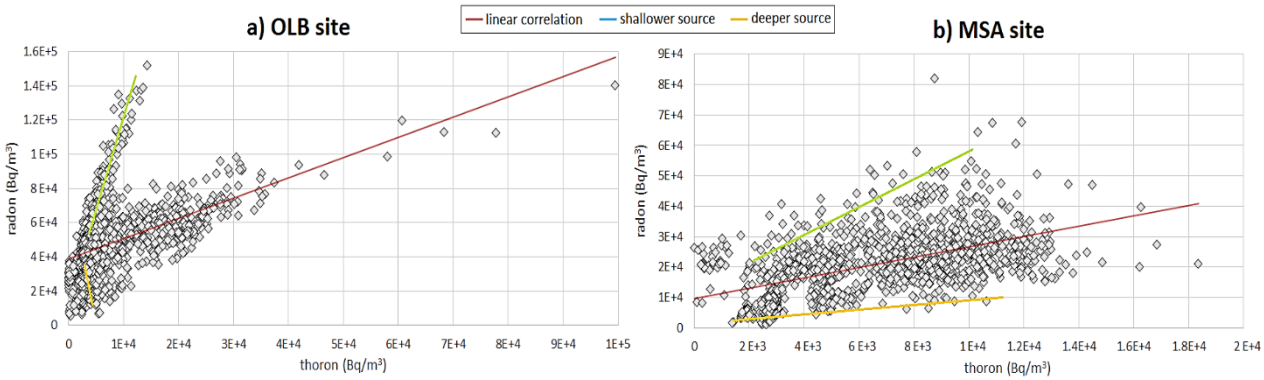

Figure 6. Activity concentration of ^{222}Rn (radon) vs. ^{220}Rn (thoron) at OLB (**a**) and MSA (**b**) sites during the monitoring period of 1 July 2011–31 December 2017. The red lines indicate a linear correlation between the two isotopes of the gas; the green and yellow lines indicate the different correlations for the parts of recorded data that should come from shallow and deep sources, respectively [62].

5. Conclusions

This paper focused on the study of surface soil gas ^{220}Rn (thoron) monitored during a long data series from 2011 to 2017 at two sites of the Campi Flegrei caldera, in the district of Naples, Southern Italy. Over the last two decades, the Campi Flegrei caldera has been in an unrest phase characterized by ground uplift, seismicity, fumarolic degassing and a general increase in the emission of volcanic–hydrothermal fluids. Based on a previous similar work centered on ^{222}Rn, the major radon isotope, which highlights a remarkable correlation with geo-indicators used to characterize the caldera unrest, here, the main objective was to verify whether and how this volcanically induced crisis might also affect the ^{220}Rn activity concentration in the surface soils, considering that its surface exhalation rate is influenced by external factors, which can also act at a distance from the measuring point in these particular areas. The results of the study show that ^{220}Rn presents an increasing pattern very similar to that of the more classic geophysical and geochemical parameters routinely monitored during the evolution of volcanic systems, as well as the ^{222}Rn. The strong increase in temperature and pressure alterations of the hydrothermal system of Campi Flegrei acts as a perturbation significantly affecting the surface thoron emanation power, favored by the high permeability and porosity of the rocks. The carrier effects, due to CO_2 gas fluxes, may further enrich the gas emission phenomenon. In fact, ^{222}Rn and ^{220}Rn highlight a general good linear correlation due to the CO_2 carrier action, although small effects of different Rn gas sources, likely from a quiet period of hydrothermal and seismic activity, are present. These results represent an absolute novelty in the study of the ^{220}Rn isotope, as it is very rarely used in geophysical studies, due to its very short half-life of 55.6 s. The long-term observation of ^{220}Rn at multiple sites in surface soils of a seismic–volcanic area can improve the understanding and use of the short-lived isotope, at the same level of the most mentioned in the literature and long-lived ^{222}Rn. A further simple positive advantage in using thoron instead of or together with radon measurements could be in the context of low-cost large-area monitoring; since the ^{212}Po progeny of ^{220}Rn bears the highest naturally occurring alpha particle energy (almost 8.8 MeV, with a more than 1 MeV-large gap to the next ^{214}Po), it could be more easily distinguished from other alpha decays.

Author Contributions: Conceptualization, F.A. and C.S.; methodology, F.A.; software, F.A.; validation, F.A., C.S. and V.R.; formal analysis, F.A.; investigation, F.A. and C.S.; resources, F.A. and C.S.; data curation, V.R., F.G., W.D.C. and M.P.; writing—original draft preparation, F.A. and C.S.; writing—review and editing, F.A., C.S., V.R., F.G., W.D.C. and M.P.; visualization, F.A., C.S., V.R. and F.G.; supervision, F.A., C.S. and V.R.; project administration, F.A., and C.S.; funding acquisition, C.S., V.R. and F.G. All authors have read and agreed to the published version of the manuscript.

Funding: This research received no external funding.

Institutional Review Board Statement: Not applicable.

Informed Consent Statement: Not applicable.

Data Availability Statement: Not applicable.

Conflicts of Interest: The authors declare no conflict of interest.

References

1. Sabbarese, C.; Ambrosino, F.; Chiodini, G.; Giudicepietro, F.; Macedonio, G.; Caliro, S.; De Cesare, W.; Bianco, F.; Pugliese, M.; Roca, V. Continuous radon monitoring during seven years of volcanic unrest at Campi Flegrei caldera (Italy). *Sci. Rep.* **2020**, *10*, 9551. [CrossRef]
2. Ambrosino, F.; Sabbarese, C.; Buompane, R.; Roca, V. Development and calibration of a method for direct measurement of ^{220}Rn (thoron) activity concentration. *Appl. Radiat. Isot.* **2020**, *166*, 109310. [CrossRef]
3. Oh, Y.H.; Kim, G. A radon-thoron isotope pair as a reliable earthquake precursor. *Sci. Rep.* **2015**, *5*, 13084. [CrossRef]
4. Sabbarese, C.; Ambrosino, F.; D'Onofrio, A. Development of radon transport model in different types of dwellings to assess indoor activity concentration. *J. Environ. Radioact.* **2021**, *227*, 106501. [CrossRef]
5. Siročić, A.P.; Stanko, D.; Sakač, N.; Dogančić, D.; Trojko, T. Short-term measurement of indoor radon concentration in Northern Croatia. *Appl. Sci.* **2020**, *10*, 2341. [CrossRef]
6. Ambrosino, F.; Sabbarese, C.; Roca, V.; Giudicepietro, F.; De Cesare, W. Connection between ^{222}Rn emission and geophysical-geochemical parameters recorded during the volcanic unrest at Campi Flegrei. *Appl. Radiat. Isot.* **2020**, *166*, 109385. [CrossRef] [PubMed]
7. Pinto, P.V.; Kumara, K.S.; Karunakara, N. Mass exhalation rates, emanation coefficients and enrichment pattern of radon, thoron in various grain size fractions of monazite rich beach placers. *Radiat. Meas.* **2020**, *130*, 106220. [CrossRef]
8. Iskandar, D.; Yamazawa, H.; Iida, T. Quantification of the dependency of radon emanation power on soil temperature. *Appl. Radiat. Isot.* **2004**, *60*, 971–973. [CrossRef]
9. Garavaglia, M.; Dal Moro, G.; Zadro, M. Radon and tilt measurements in a seismic area: Temperature effects. *Phys. Chem. Earth Part A* **2000**, *25*, 233–237. [CrossRef]
10. Ghosh, D.; Deb, A.; Sengupta, R. Anomalous radon emission as precursor of earthquake. *J. Appl. Geophy.* **2009**, *69*, 67–81. [CrossRef]
11. Ambrosino, F.; Thinová, L.; Briestenský, M.; Šebela, S.; Sabbarese, C. Detecting time series anomalies using hybrid methods applied to Radon signals recorded in caves for possible correlation with earthquakes. *Acta Geod. Geophys.* **2020**, *55*, 405–420. [CrossRef]
12. Cigolini, C.; Laiolo, M.; Coppola, D.; Ulivieri, G. Preliminary radon measurements at Villarrica volcano, Chile. *J. S. Am. Earth Sci.* **2013**, *46*, 1–8. [CrossRef]
13. Bochao, X.; Dong, X.; Burnett, W.C.; Dimova, N.T.; Houjie, W.; Longjun, Z.; Maosheng, G.; Xueyan, J.; Zhigang, Y. Natural ^{222}Rn and ^{220}Rn indicate the impact of the Water-Sediment Regulation Scheme (WSRS) on submarine groundwater discharge in the Yellow River estuary, China. *Appl. Geochem.* **2014**, *51*, 79–85.
14. Hu, J.; Yang, G.; Hegedűs, M.; Iwaoka, K.; Hosoda, M.; Tokonami, S. Numerical modeling of the sources and behaviors of ^{222}Rn, ^{220}Rn and their progenies in the indoor environment—A review. *J. Environ. Radioact.* **2018**, *189*, 40–47. [CrossRef]
15. Ramola, R.C.; Prasad, M.; Kandari, T.; Pant, P.; Bossew, P.; Mishra, R.; Tokonami, S. Dose estimation derived from the exposure to radon, thoron and their progeny in the indoor environment. *Sci. Rep.* **2016**, *6*, 31061. [CrossRef]
16. Sabot, B.; Pierre, S.; Cassette, P.; Michielsen, N.; Bondiguel, S. Development of a primary thoron activity standard calibration of thoron measurement instruments. *Radiat. Prot. Dosim.* **2015**, *167*, 70–74. [CrossRef]
17. Jaishi, H.P.; Singh, S.; Tiwari, R.P.; Tiwari, R.C. Soil-gas thoron concentration associated with seismic activity. *Chiang Mai J. Sci.* **2015**, *42*, 972–979.
18. Ambrosino, F.; Sabbarese, C.; Roca, V.; Giudicepietro, F.; Chiodini, G. Analysis of 7-years radon time series at Campi Flegrei area (Naples, Italy) using artificial neural network method. *Appl. Radiat. Isot.* **2020**, *163*, 109239. [CrossRef] [PubMed]
19. Tamburrello, G.; Caliro, S.; Chiodini, G.; De Martino, P.; Avino, R.; Minopoli, C.; Carandente, A.; Rouwet, D.; Aiuppa, A.; Costa, A.; et al. Escalating CO_2 degassing at the pisciarelli fumarolic system, and implications for the ongoing Campi Flegrei unrest. *J. Volcanol. Geotherm. Res.* **2019**, *384*, 151–157. [CrossRef]
20. Chiodini, G.; Caliro, S.; Cardellini, C.; Granieri, D.; Avino, R.; Baldini, A.; Donnini, M.; Minopoli, C. Long-term variations of the Campi Flegrei, Italy, volcanic system as revealed by the monitoring of hydrothermal activity. *J. Geophys. Res.* **2010**, *115*, B03205. [CrossRef]
21. Del Gaudio, C.; Aquino, I.; Ricciardi, G.P.; Ricco, C.; Scandone, R. Unrest episodes at Campi Flegrei: A reconstruction of vertical ground movements during 1905–2009. *J. Volcanol. Geotherm. Res.* **2010**, *195*, 48–56. [CrossRef]
22. Trasatti, E.; Polcari, M.; Bonafede, M.; Stramondo, S. Geodetic contraints to the source mechanism of the 2011–2013 unrest at Campi Flegrei (Italy) caldera. *Geoph. Res. Lett.* **2015**, *42*, 3847–3854. [CrossRef]

23. Cardellini, C.; Chiodini, G.; Frondini, F.; Avino, R.; Bagnato, E.; Caliro, S.; Lelli, M.; Rosiello, A. Monitoring diffuse volcanic degassing during volcanic unrests: The case of Campi Flegrei (Italy). *Sci. Rep.* **2017**, *7*, 6757. [CrossRef] [PubMed]
24. Ambrosino, F.; Thinová, L.; Briestenský, M.; Sabbarese, C. Anomalies identification of Earth's rotation rate time series (2012–2017) for possible correlation with strong earthquakes occurrence. *Geod. Geodyn.* **2019**, *10*, 455–459. [CrossRef]
25. Du, P.; Wang, J.; Yang, W.; Niu, T. Multi-step ahead forecasting in electrical power system using a hybrid forecasting system. *Renew. Energy* **2018**, *122*, 533–550. [CrossRef]
26. Ambrosino, F.; Thinová, L.; Hýža, M.; Sabbarese, C. ^{214}Bi/^{214}Pb radioactivity ratio three-year monitoring in rainwater in Prague. *Nukleonika* **2020**, *65*, 115–119. [CrossRef]
27. Ambrosino, F.; De Cesare, W.; Roca, V.; Sabbarese, C. Mathematical and geophysical methods for searching anomalies of the radon signal related to earthquakes. *J. Phys. Conf. Ser.* **2019**, *1226*, 012025. [CrossRef]
28. Ambrosino, F.; Stellato, L.; Sabbarese, C. A case study on possible radiological contamination in the Lo Uttaro landfill site (Caserta, Italy). *J. Phys. Conf. Ser.* **2020**, *1548*, 012001. [CrossRef]
29. Ambrosino, F.; Buompane, R.; Pugliese, M.; Roca, V.; Sabbarese, C. RaMonA system for radon and thoron measurement. *Nuovo Cimento C* **2018**, *41*, 222.
30. Sabbarese, C.; Ambrosino, F.; Buompane, R.; Pugliese, M.; Roca, V. Analysis of alpha particles spectra of the radon and thoron progenies generated by an electrostatic collection detector using new software. *Appl. Radiat. Isot.* **2017**, *122*, 180–185. [CrossRef]
31. Endo, E.T.; Murray, T. Real-time seismic amplitude measurement (RSAM): A volcano monitoring and prediction tool. *Bull. Volcanol.* **1991**, *53*, 533–545. [CrossRef]
32. Chiodini, G.; Selva, J.; Del Pezzo, E.; Marsan, D.; De Siena, L.; D'Auria, L.; Bianco, F.; Caliro, S.; De Martino, P.; Ricciolino, P.; et al. Clues on the origin of post-2000 earthquakes at Campi Flegrei caldera (Italy). *Sci. Rep.* **2017**, *7*, 4472. [CrossRef] [PubMed]
33. Giudicepietro, F.; Chiodini, G.; Caliro, S.; De Cesare, W.; Esposito, A.M.; Galluzzo, D.; Lo Bascio, D.; Macedonio, G.; Orazi, M.; Ricciolino, P.; et al. Insight into Campi Flegrei caldera unrest through seismic tremor measurements at Pisciarelli fumarolic field. *Geochem. Geophys. Geosystems* **2019**, *20*, 5544–5555. [CrossRef]
34. Caliro, S.; Chiodini, G.; Moretti, R.; Avino, R.; Granieria, D.; Russo, M.; Fiebig, J. The origin of the fumaroles of La Solfatara (Campi Flegrei, South Italy). *Geochim. Cosmochim. Acta* **2007**, *71*, 3040–3055. [CrossRef]
35. Chiodini, G.; Giudicepietro, F.; Vandemeulebrouck, J.; Aiuppa, A.; Caliro, S.; De Cesare, W.; Tamburello, G.; Avino, R.; Orazi, M.; D'Auria, L. Fumarolic tremor and geochemical signals during a volcanic unrest. *Geology* **2017**, *45*, 1131–1134. [CrossRef]
36. Wang, J.; Yang, W.; Du, P.; Li, Y. Research and application of a hybrid forecasting framework based on multi-objective optimization for electrical power system. *Energy J.* **2018**, *148*, 59–78. [CrossRef]
37. Sabbarese, C.; Ambrosino, F.; De Cicco, F.; Pugliese, M.; Quarto, M.; Roca, V. Signal decomposition and analysis for the identification of periodic and anomalous phenomena in Radon time-series. *Radiat. Prot. Dosim.* **2017**, *177*, 202–206. [CrossRef]
38. Ambrosino, F.; Thinová, L.; Briestenský, M.; Giudicepietro, F.; Roca, V.; Sabbarese, C. Analysis of geophysical and meteorological parameters influencing ^{222}Rn activity concentration in Mladeč caves (Czech Republic) and in soils of Phlegrean Fields caldera (Italy). *Appl. Radiat. Isot.* **2020**, *160*, 109140. [CrossRef]
39. Hong, L. Decomposition and forecast for financial time series with high-frequency based on Empirical Mode Decomposition. *Energy Procedia* **2011**, *5*, 1333–1340. [CrossRef]
40. Kim, D.; Oh, H.S. Empirical mode decomposition with missing values. *Springerplus* **2016**, *5*, 2016. [CrossRef]
41. Duan, W.Y.; Han, Y.; Huang, L.M.; Zhao, B.B.; Wang, M.H. A hybrid EMD-SVR model for the short-term prediction of significant wave height. *Ocean Eng.* **2016**, *124*, 54–73. [CrossRef]
42. Sousa, J.C.; Jorge, H.M.; Neves, L.P. Short-term load forecasting based on support vector regression and load profiling. *Int. J. Energy Res.* **2014**, *38*, 350–362. [CrossRef]
43. Baldacci, L.; Golfarelli, M.; Lombardi, D.; Sami, F. Natural gas consumption forecasting for anomaly detection. *Expert Syst. Appl.* **2016**, *62*, 190–201. [CrossRef]
44. Ambrosino, F.; Thinová, L.; Briestenský, M.; Sabbarese, C. Analysis of radon time series recorded in Slovak and Czech caves for the detection of anomalies due to seismic phenomena. *Radiat. Prot. Dosim.* **2019**, *186*, 428–432. [CrossRef] [PubMed]
45. Kuo, T.; Chen, W.; Ho, C. Anomalous decrease in groundwater radon before 2016 Mw 6.4 Meinong earthquake and its application in Taiwan. *Appl. Radiat. Isot.* **2018**, *136*, 68–72. [CrossRef] [PubMed]
46. Alexandrov, T.; Bianconcini, S.; Dagum, E.B.; Maass, P.; McElroy, T.S. A review of some modern approaches to the problem of trend extraction. *Econom. Rev.* **2012**, *31*, 593–624. [CrossRef]
47. Ambrosino, F.; Pugliese, M.; Roca, V.; Sabbarese, C. Innovative methodologies for the analysis of radon time series. *Nuovo Cimento C* **2018**, *41*, 223.
48. Chiodini, G.; Paonita, A.; Aiuppa, A.; Costa, A.; Caliro, S.; De Martino, P.; Acocella, V.; Vandemeulebrouck, J. Magmas near the critical degassing pressure drive volcanic unrest towards a critical state. *Nat. Commun.* **2016**, *7*, 13712l. [CrossRef] [PubMed]
49. Bonaccorso, A.; Currenti, G.; Del Negro, C.; Boschi, E. Dike deflection modelling for inferring magma pressure and withdrawal, with application to Etna 2001 case. *Earth Planet. Sci. Lett.* **2010**, *293*, 121–129. [CrossRef]
50. Chiodini, G.; Marini, L. Hydrothermal gas equilibria: The H_2O-H_2-CO_2-CO-CH_4 system. *Geochim. Cosmochim. Acta* **1998**, *62*, 2673–2687l. [CrossRef]
51. Etiope, G.; Martinelli, G. Migration of carrier and trace gases in the geosphere: An overview. *Phys. Earth Planet. Inter.* **2002**, *129*, 185–204. [CrossRef]

52. Giammanco, S.; Sims, K.W.W.; Neri, M. Measurements of ^{220}Rn and ^{222}Rn and CO_2 emissions in soil and fumarole gases on Mt. Etna volcano (Italy): Implications for gas transport and shallow ground fracture. *Geochem. Geophys. Geosyst.* **2007**, *8*, Q10001. [CrossRef]
53. Voltattorni, N.; Lombardi, S.; Rizzo, S. ^{222}Rn and CO_2 soil-gas geochemical characterization of thermally altered clays at Orciatico (Tuscany, Central Italy). *Appl. Geochem.* **2010**, *25*, 1248–1256. [CrossRef]
54. Rodrigo-Naharro, J.; Quindós, L.S.; Clemente-Jul, C.; Mohamud, A.H.; del Villara, L.P. CO_2 degassing from a Spanish natural analogue for CO_2 storage and leakage: Implications on ^{222}Rn mobility. *Appl. Geochem.* **2017**, *84*, 297–305. [CrossRef]
55. Mollo, S.; Tuccimei, P.; Galli, G.; Iezzi, G.; Scarlato, P. The imprint of thermally induced devolatilization phenomena on radon signal: Implications for the geochemical survey in volcanic areas. *Geophys. J. Int.* **2017**, *211*, 558–571. [CrossRef]
56. Domingos, F.; Pereira, A. Implications of alteration processes on radon emanation, radon production rate and W-Sn exploration in the Panasqueira ore district. *Sci. Total Environ.* **2018**, *622–623*, 825–840. [CrossRef]
57. Sabbarese, C.; Ambrosino, F.; D'Onofrio, A.; Pugliese, M.; La Verde, G.; D'Avino, V.; Roca, V. The first radon potential map of the Campania region (Southern Italy). *Appl. Geochem.* **2021**, *126*, 104890. [CrossRef]
58. Aiuppa, A.; Tamburello, G.; Di Napoli, R.; Cardellini, C.; Chiodini, G.; Giudice, G.; Grassa, F.; Pedone, M. First observations of the fumarolic gas output from a restless caldera: Implications for the current period of unrest (2005–2013) at Campi Flegrei: Fumarolic gas output from Campi Flegrei. *Geochem. Geophys. Geosyst.* **2013**, *14*, 4153–4169. [CrossRef]
59. Sabbarese, C.; Ambrosino, F.; D'Onofrio, A.; Roca, V. Radiological characterization of natural building materials from the Campania region (Southern Italy). *Constr. Build. Mater.* **2021**, *268*, 121087. [CrossRef]
60. Cigolini, C.; Salierno, F.; Gervino, G.; Bergese, P.; Marino, C.; Russo, M.; Prati, P.; Ariola, V.; Bonetti, R.; Begnini, S. High-resolution radon monitoring and hydrodynamics at Mount Vesuvius. *Geophys. Res. Lett.* **2001**, *20*, 4035–4038. [CrossRef]
61. D'Alessandro, W.; Parello, F. Soil gas prospection of He, ^{222}Rn and CO_2: Vulcano Porto area, Aeolian Islands, Italy. *Appl. Geochem.* **1997**, *12*, 213–224. [CrossRef]
62. Yang, T.F.; Walia, V.; Chyi, L.L.; Fu, C.C.; Chen, C.H.; Liu, T.K.; Song, S.R.; Lee, C.Y.; Lee, M. Variations of soil radon and thoron concentrations in a fault zone and prospective earthquakes in SW Taiwan. *Radiat. Meas.* **2005**, *40*, 496–502. [CrossRef]